Available online at www.sciencedirect.com
SCIENCE DIRECT®
Journal of Photochemistry and Photobiology A: Chemistry 164 (2004) 193–198
Journal of Photochemistry and Photobiology A:Chemistry
www.elsevier.com/locate/jphotochem

100 mm × 100 mm large-sized dye sensitized solar cells

Kenichi Okada*, Hiroshi Matsui, Takuya Kawashima, Tetsuya Ezure, Nobuo Tanabe

Electronics Material Department, Material Technology Laboratory, Fujikura Limited, 1-5-1 kiba, Koto-ku, Tokyo 135-8512, Japan

Received 25 July 2003; received in revised form 1 December 2003; accepted 4 January 2004

Abstract

In this study, up sizing technology of dye sensitized solar cells (DSC) was developed. Conversion efficiency of large cells was drastically decreased if it was fabricated by ordinary materials and processes of mini size cells, due to its high internal resistance. We investigated a method to reduce sheet resistant of transparent conductive substrates. It was found that nickel was appropriate for current correcting lines of DSCs because of its lifetime in a redox electrolyte, and low dark current density to the electrolyte. High conductive transparent substrates were fabricated with nickel grids formed by an electroplating process and fluorine doped SnO_2/ITO double layered transparent conductive oxides. These substrates achieved low sheet resistance 0.28 Ω/□ and 66% light transmittance, and 4.3% conversion efficiency in the total area, 5.1% in the active area was obtained on a 100 mm × 100 mm size large cell.

Keywords: Dye sensitized solar cells; Metal grid; Large modules

1. Introduction

Dye sensitized solar cells (DSC) are expected to become popular solar cells because of their advantages of cost and efficiency. Several technologies to bring practical performance of life and cost of DSC modules have been investigated recently. For example, studies of ionic liquid electrolytes [1,2], quasi-solids [3–5] and solid hole transfer materials [6] are investigated to realize long-life and safe DSC modules. Studies of low-temperature fabrication of TiO_2 on a flexible conductive film [7–9] is investigated to realize a high-speed and low-cost manufacturing process of DSC modules. Up sizing of DSC modules is also one of the important technologies to bring about commercialization of DSCs.

Cell size and conductivity of substrates influence the internal resistance of solar cells; it consequently influences the fill factor and conversion efficiency of them. For that reason, small size cells are normally used to obtain high conversion efficiency on non-industrial studies, but the efficiency of 0.3% was very low when 100 mm × 100 mm large cell was fabricated with a 10 Ω/□ fluorine doped SnO_2 (FTO) substrate normally used for mini size cells.

To enlarge cell sizes, several processes were attempted. There are two groups of design types. The first is large size modules, which are formed by aligned and connected small or narrow rectangular cells in series [10–12]. This type of module may have two advantages. Each constituent cell can be fabricated with optimized processes for high performance mini size DSCs, and high open circuit voltage, which is indispensable to drive electric devices, can be obtained from a single module.

The second is the large single cell that is made with high electric conductive substrates [12–15]. These modules are expected to have high productivity because of their simple module structures [14], and installation area of cell modules is expected to be small because of their high aperture ratio. We think that the single cell type large module is more advisable for DSCs of outdoor applications, since their simple structure will make full use of DSC advantages of cost and efficiency.

Commercial solar cells like poly-crystalline Si solar cells have a current-collecting grid that was made by silver solder or conductive printing paste to reduce their high surface resistance. In case of DSC, these materials cannot be adopted, since these materials are attacked by I^-/I_3^- redox electrolytes [14], and charge recombination between metal grids and redox electrolytes reduces photocurrent of the cells. Although there are some precedents for protecting the metal grid from redox electrolytes by resin [12,13] or glass-ceramic [14,15], fabrication processes of DSC will

* Corresponding author. Tel.: +81-3-5606-1067; fax: +81-3-5606-1511.
E-mail addresses: k_okada@rd.fujikura.co.jp (K. Okada), matsui@rd.fujikura.co.jp (H. Matsui), kawasima@rd.fujikura.co.jp (T. Kawashima), t_ezure@fujikura.co.jp (T. Ezure), ntanabe@rd.fujikura.co.jp (N. Tanabe).

1010-6030/$ – see front matter © 2004 Elsevier B.V. All rights reserved.
doi:10.1016/j.jphotochem.2004.01.028

become simpler if metal grids are fabricated with low dark current, heat and electrolyte resistant materials.

In this study, we investigated low dark current materials for the current collecting grid, and examined their weight losses in a redox electrolyte. A high electric conductive substrate with metal grids was designed, and fabricated by a manufacturing process for a printed wiring board. 100 mm × 100 mm large cells, the same size as commercial solar cells, were fabricated with these substrates.

2. Experimental

2.1. Evaluation of grid metals

Weight loss rates of metals in an I^-/I_3^- redox electrolyte were measured with the following procedure. Several kinds of metal thin films were formed on 1.0 cm × 2.5 cm glass substrates by magnetron rf sputter deposition as immersion sample pieces. Deposition thickness of films were controlled to be 500 nm. These sample pieces were calcined at 450 °C in air for 1 h; the same condition as the solar cell preparation process. Every two sample pieces were immersed in an 80 °C × 20 cm^3 redox electrolyte in sealed test tubes, and weight losses were measured after 1, 6, 24, 100, 400 and 1600 h periods. The I^-/I_3^- redox electrolyte consisted of 0.05 M I_2, 0.1 M LiI, 0.3 M 1,2-dimethyl-3-propylimidazolium iodide and 0.5 M *tert*-butylpyridine in methoxy acetonitrile.

Current from the I^-/I_3^- redox electrolyte to a metal electrode was evaluated with the following procedure by a simple cell set shown in Fig. 1 to compare dark current change of DSC if metal grids were placed on a photoelectrode, since it was difficult to measure the reduction current of metals with the three electrode method using a reference electrode in high concentration I^-/I_3^- electrolytes. 1.4 cm × 2 cm metal electrode samples were prepared by the same process as the immersion test samples. These samples and the same sized Pt counter electrodes made by sputter deposition were clamped together with 50 μm thickness sheets of ionomer resin (HIMILAN, Du Pont-Mitsui Polychemicals) as sealant and spacer, so that the active area became 1 cm × 1 cm. The redox electrolyte was injected into the test cell gap through a prepared pinhole in the counter electrodes and sealed before measuring. These sample pieces had the same dimensions and fabrication processes as the mini size DSC cells, except for a nanoporous TiO_2 layer fabrication process. Relationships between dark current and bias voltage of the test cells were measured using a dc power source (SI1286, Schlumberger Technologies).

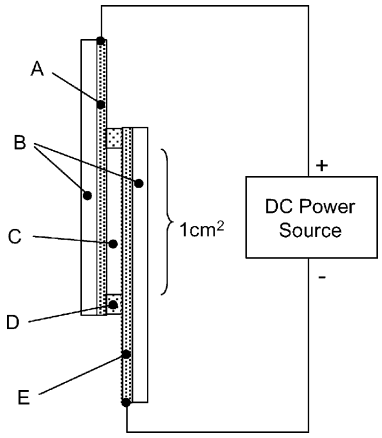

Fig. 1. Cross-sectional design of the sample cell and connection of test equipments: (A) is the Pt counter electrode, (B) is the FTO conductive glass substrate, (C) is the I^-/I_3^- redox electrolyte, (D) is the ionomer sealing resin and (E) is the sample metal film.

2.2. Metal grid fabrication

Fig. 2 shows a design of a substrate with metal grids for the large size DSC. Metal grids were formed on a glass substrate directly by the additive process. The additive process is known as a photolithographic manufacturing process for printed wiring boards of which patterned metal lines are formed by electroplating. Scheme 1 shows a flow diagram of the additive process for the substrate with metal grids, and materials and preparation conditions are shown in Table 1. A 100 nm Cr layer was prepared on a glass substrate by rf magnetron sputter deposition as an electroplating seed layer (Scheme 1: a). A metal grid pattern was formed by photosensitive dry film resist on a substrate so that its grid aperture ratio became 85% (Scheme 1: b and c), and a Ni layer was electroplated on the patterned substrate (Scheme 1: d). The average Ni grid thickness was 2.0 μm. Although a larger Ni grid thickness was desirable

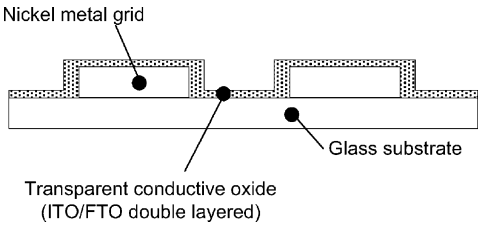

Fig. 2. Cross-sectional design of the transparent conductive glass with nickel metal grids. Line widths are 2 mm and 200 μm, aperture ratio is 85%, Ni thickness is 2 μm and FTO/ITO thickness is 0.6 μm.

Table 1
Materials and preparation conditions of Ni grid substrates

Substrate		TEMPAX#8330, Schott 100 mm × 100 mm × 1.1 mm (*t*)
Dry film resist		AQ1558, Asahi Kasei
Ni electroplating	Condition bath	50 °C, 2.0 A/dm^2 × 6.3 min (2 μm) 1.8 M: nickel(II) sulfamate[a] 0.04 M: nickel(II) chloride 0.57 M: boric acid 3 ml/l: pit preventing agent[b]

[a] Nihon Kagaku Sangyo.
[b] Acna-H (Okuno Chemical Industries).

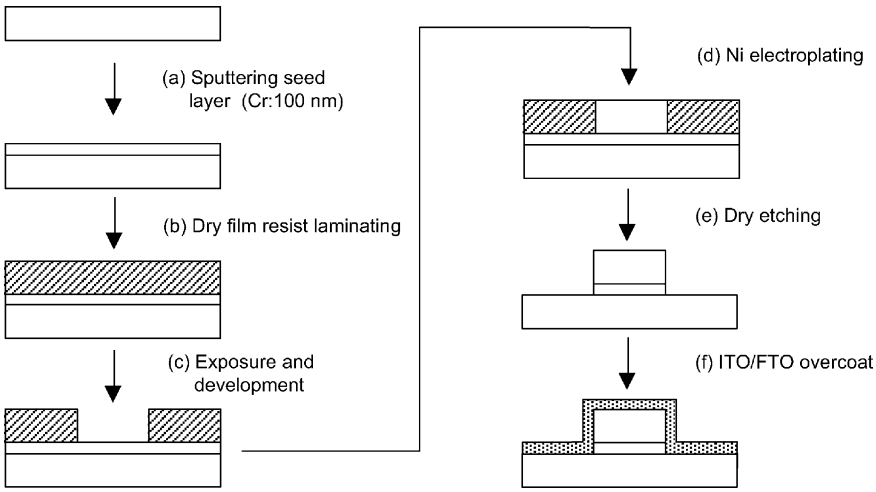

Scheme 1. The additive manufacturing process of metal grid on a glass substrate.

to increase the aperture ratio, the Ni thickness could not become thicker than 2.0 μm on the glass because of the high contractile force after the 450 °C × 30 min calcining process. The Cr seed layer was removed after Ni electroplating by dry etching (Scheme 1: e). Fig. 3 shows a Ni metal grid formed by these procedures. An FTO, indium tin oxide (ITO) double layered transparent conductive oxide (FTO/ITO) was formed on the substrates by the spray pyrolysis deposition method (Scheme 1: f) [16]. This layer was expected to have two functions, one is collecting photocurrent from the inter-grid area, and the other is protecting metal grids from redox electrolytes, although it is imperfect.

2.3. Solar cell fabrication procedure

To avoid delamination, colloidal TiO_2 paste was prepared with two types of nanoparticles. The paste consisted of 80 wt.% TiO_2 colloidal printing paste (Ti nanoxide-T, Solaronix SA) and 20 wt.% colloidal suspension [17] containing 15 wt.% TiO_2 nanoparticles (P25, Nippon Aerosil). Nanoporous TiO_2 layers were made from the printing paste using a doctor-blading technique on the metal grid formed conductive substrates by sintering at 450 °C in air for 30 min.

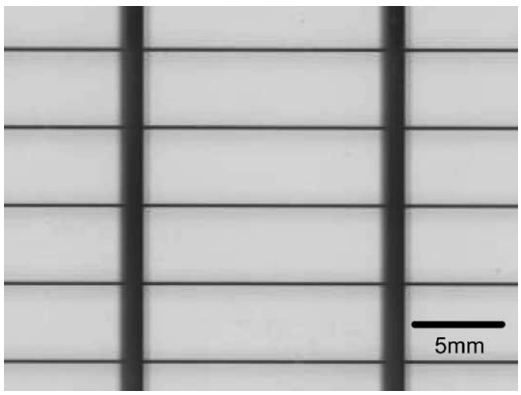

Fig. 3. A microscopic image of Ni metal grids on a glass substrate.

Subsequently, the suspension of larger size TiO_2 particles (~200 nm in diameter, Junsei Chemical) was coated on the nanoporous layer as a light reflecting layer using the same procedure.

The Nanoporous TiO_2 layers were immersed a mixed solvent of 50 wt.% butanol and 50 wt.% acetonitrile containing 0.3 mM Ru-dye (*cis*-di(thiocyanato)-bis(2,2′-bipyridine-4,4′-dicalboxylic acid)ruthenium(II) (known as N3 dye) for 18 h at room temperature. Pt counter electrodes were prepared by the sputter deposition method on transparent conductive glasses. A thick Pt layer of 4.0 μm was formed as the counter electrode to decrease the sheet resistance, and the measured sheet resistances of Pt counter electrodes were 0.1 Ω/□. Solar cells were made by placing the counter electrode on the photoelectrode and then the redox electrolyte was introduced from the edges of the two electrodes. They were adhered together by the atmospheric pressure through the measurement. The photocurrent–voltage characteristics of the solar cells were measured using a dc power source (SI1286, Schlumberger Technologies) and a dc electronic load (MP-160, Eiko Seiki) under the AM 1.5 simulated light (ESS-150A, Eiko Seiki).

3. Result and discussion

3.1. Evaluation of grid metals

Fig. 4 shows the results of the immersion test of six metal thin films in the I^-/I_3^- redox electrolyte. Au and Ag films had a very high weight loss rate and films disappeared after 1 h. Al films lost their metallic luster and became aluminum oxide after 100 h of sintering. Compared with these metals, weight losses of Pt, Ti and Ni films were lower. The time for the disappearance of metal films in the immersion test are summarized in Table 2. It is desirable that grid metals of practical solar cells have longer lifetime than Pt thin film which is a standard material for counter electrodes for DSCs.

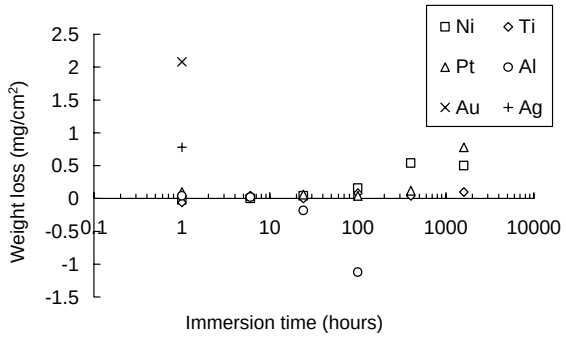

Fig. 4. The relationships between weight losses of metal thin films on glasses and immersion time in 20 ml × 80 °C I^-/I_3^- redox electrolytes. The values are average of $N = 2$. The sample dimensions were 10 mm × 25 mm × 0.5 μm (t), and every two sample pieces were immersed in a test tube.

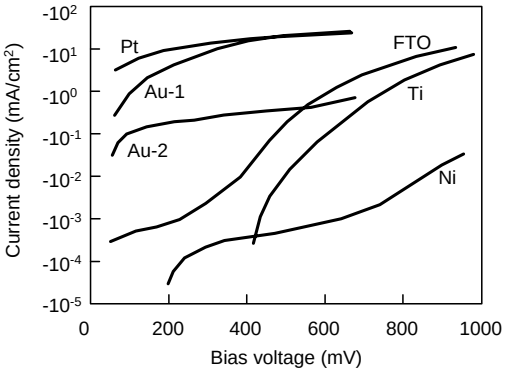

Fig. 5. The relationships between bias voltage and the dark current of sample cells with each metal layer. (Au-1) is the bare Au sample, (Au-2) is the Au sample with 200 nm overcoated TiO_2 layer and (FTO) is the blank sample without metal layer.

Table 2
The time for the disappearance of sputter deposited 10 mm × 25 mm × 0.5 μm (t) × 2 thin metal films in 20 ml × 80 °C I^-/I_3^- redox electrolyte

Metal species	Time for the disappearance (h)
Au	<1
Ag	<1
Al	100
Pt	1600
Ni	>1600
Ti	>1600

Fig. 5 shows the dark current of sample cells with each metal layer. Pt and Au had a very high dark current. When these materials are used, solar cells must have very low conversion efficiency because of large photocurrent recombination. To reduce electron transfer between the surface of metal and the electrolyte, a 0.2 μm TiO_2 overcoat layer was formed on an Au film sample by rf sputter deposition. Although the coated Au layer had 1/10–1/100 dark current compared with bare Au, the coated sample had a larger dark current than that of FTO. The overcoated TiO_2 layer might have a few micro-pores or micro cracks that grew through the 450 °C × 30 min calcining process, due to the difference of expansion coefficient. These micro defects may also be the cause of grid corrosion if it is fabricated by weak metals in redox electrolytes. Ti and Ni had a lower dark current than the FTO. Probably, these metals do not cause photocurrent recombination losses, and large size solar cells fabricated with these metals are expected to show high conversion efficiency.

Fig. 6 shows electric resistivity and the dark current of each metal when their bias voltages were 500 mV. Low electric resistivity of the grid metal is desirable to ensure a high aperture ratio and low sheet resistance of substrates. Moreover, a dark current from the metal layer that is less than that from the FTO is required to ensure high conversion efficiency. Besides these three properties, the process cost becomes a considerable merit for grid materials when it is applied to commercial solar cells. For example, there is no low cost process for titanium to fabricate grids on a glass, although Ti films have a long lifetime. In consideration of these results, it was thought that Ni film was an applicable

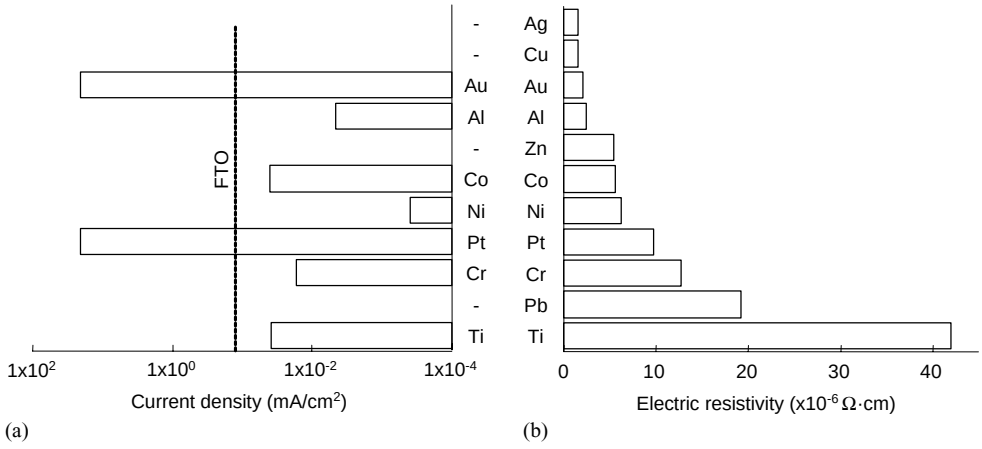

Fig. 6. The dark current of each metal layer when their bias voltages were 500 mV (a) and electric resistivity of metals (b) [18]. (FTO) is the dark current of FTO substrate and (−) is not measured.

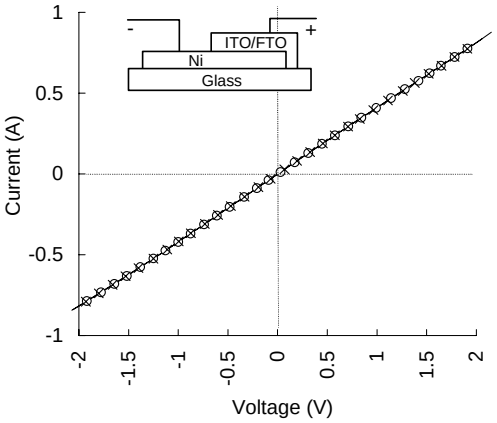

Fig. 7. Current–voltage characteristics of the junction between the FTO/ITO layer and the Ni layer. Dimensions of the Ni layer is 5 mm × 100 mm × 0.5 μm (*t*), FTO/ITO is overcoated on 5 mm × 50 mm area and inter-probe length is 40 mm. (○) as-deposited and (×) after 450 °C × 30 min.

grid material for DSCs. Fig. 7 shows current–voltage characteristics of a junction between an FTO/ITO conductive oxide and a Ni layer. The current and voltage had an ohmic relationship, and the sample had almost the same characteristics after the 450 °C × 30 min calcining process. Table 3 shows sheet resistances of a Ni layer, an FTO/ITO layer and an FTO/ITO coated Ni layer. The combined sheet resistance of Ni and FTO/ITO calculated from their individual sheet resistances was almost equal to the measured sheet resistance of an FTO/ITO coated Ni layer. This shows that the contact resistance of an interface between a Ni layer and an FTO/ITO was sufficiently low, compared with their sheet resistances. From these results, it was expected that the Ni grids shown in Fig. 2 could collect photocurrent through the FTO/ITO layer normally without a large influence of electric barriers and contact resistances.

3.2. Performance of large size solar cells

The FTO/ITO conductive glass substrates with Ni grids were fabricated by the additive process for the photoelectrode. Fig. 8 shows a DSC made using an electrode with a Ni grid. The measured sheet resistance of the Ni grid was 0.049 Ω/□, and its aperture ratio was 85%. The measured sheet resistance of the FTO/ITO layer was 2.0 Ω/□,

Table 3
Individual and combined sheet resistances of Ni layer and FTO/ITO layer

	As-deposited (Ω/□)	After 450 °C × 30 min (Ω/□)
Ni layer: R_1	0.30	0.31
FTO/ITO layer: R_2	4.8	4.7
Ni + FTO/ITO (measured)	0.27	0.27
Ni + FTO/ITO (calculated)[a]	0.28	0.29

Sample size is 50 mm × 5 mm. Thickness of Ni is 0.5 μm and FTO/ITO is 0.6 μm.

[a] $1/R = 1/R_1 + 1/R_2$.

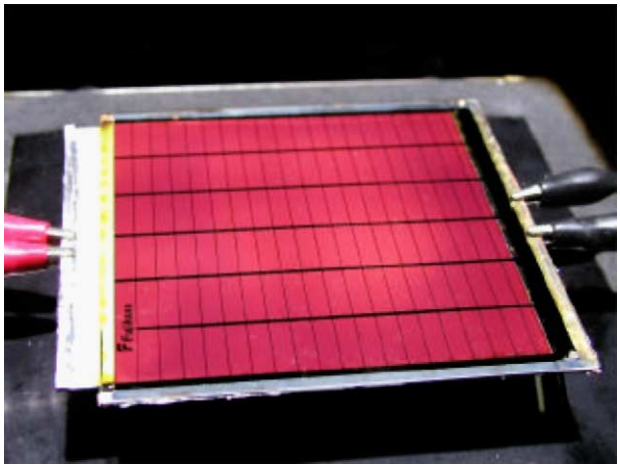

Fig. 8. The Ni grid formed large size DSC.

and its light transmittance was 78%. The combined sheet resistance of this substrate, calculated from these individual sheet resistances of grids and FTO/ITO, was 0.28 Ω/□, and the estimated total light transmittance of this substrate, including the shadow area, was 66%. The active photovoltaic conversion area was 68.9 cm^2, since the porous TiO_2 layer was fabricated in a 90 mm × 90 mm area. Fig. 9 shows the photocurrent–voltage characteristics of a large cell made with the Ni grid substrate, a large cell made with the ordinary FTO substrate for amorphous Si solar cells (Asahi, A110U80 FTO glass, 9.4 Ω/□) and a 5 mm × 9 mm mini size cell made with the ordinary FTO substrate. Fig. 10 shows the relationships between cell sizes and conversion efficiencies

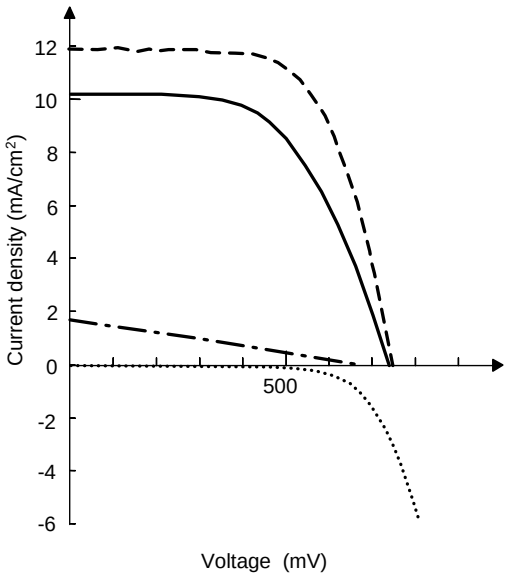

Fig. 9. Photocurrent–voltage characteristics of the 100 mm × 100 mm Ni grid large size cell (—), a 5 mm × 9 mm mini size cell (- - -), a 100 mm × 100 mm non-grid large cell (···) and dark current density of the Ni grid large cell (–·–) under AM1.5, 100 mW/cm^2. Conversion efficiency of the Ni grid large cell is 4.3% (5.1% in active area), the mini size cell is 5.7% and the non-grid large cell is 0.3%.

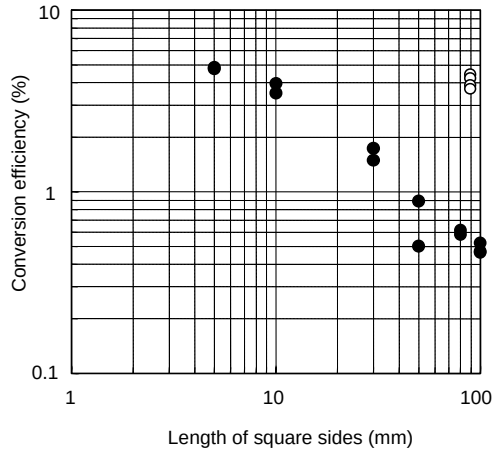

Fig. 10. The relationships between cell sizes and conversion efficiencies of (○) square DSCs using FTO/ITO substrates with Ni grids and (●) square DSCs using ordinary FTO substrates.

of ordinary FTO cells and Ni grid large cells. The conversion efficiency of the Ni grid large cell attained was 4.3% in a total area of 81 cm^2. It was corresponding to 5.1% in active area. This value was very high, compared with the large cell with the ordinary substrate, and it was approaching 90% of the mini size cell. In addition, the dark current density of the Ni grid large cell was normal. It was expected that the difference of conversion efficiency between the Ni grid large cell and the mini size cell was caused by partial unevenness of the nanoporous TiO_2 layer and distance between two electrodes.

4. Conclusions

It was found that DSC had a lower dark current density if several metals such as Ni and Ti were placed on the photoelectrode. Considering lifetimes and process costs, Ni was most applicable to grid metals of DSC substrates. Very low sheet resistance substrates for DSCs were fabricated using a FTO/ITO double-layered conductive oxide and Ni grid formed by an additive method for printed wiring boards. This substrate had a low dark current density the same as FTO, 0.28 Ω/□ low sheet resistance and 66% light transmittance. A 5.1% conversion efficiency in the active area of 68.9 cm^2 was achieved on the 100 mm × 100 mm large size cell with these substrates. For commercialization of DSCs, the conversion efficiency of 5.1% is still insufficient, but in this study, we had to use the mixture of TiO_2 paste to avoid delamination due to unevenness of the TiO_2 layer thickness. Development of the delamination-free and high-quality printing paste will be important hereafter.

Acknowledgements

This work was partially supported by New Energy and Industrial Technology Development Organization (NEDO) under Japanese government.

References

[1] N. Papageorgiou, Y. Athanassov, M. Armand, P. Bonhôte, H. Pattersson, A. Azam, M. Grätzel, J. Electrochem. Soc. 143 (1996) 3099.
[2] H. Matsumoto, T. Matsuda, T. Tsuda, R. Hagiwara, Y. Ito, Y. Miyazaki, Chem. Lett. (2001) 26.
[3] W. Kubo, T. Kitamura, K. Hanabusa, Y. Wada, S. Yanagida, Chem. Commun. 4 (2002) 374.
[4] S. Mikoshiba, H. Sumino, M. Yonetsu, S. Hayase, in: Proceedings of the 16th European Photovoltaic Solar Energy Conference, Glasgow, 2000, p. 47.
[5] H. Sumino, S. Murai, S. Mikoshiba, Toshiba Rev. 56 (2001) 7.
[6] K. Tennakone, G.R.R.A. Kumara, I.R.M. Kottegoda, K.G.U. Wijayantha, V.P.S. Perera, J. Phys. D: Appl. Phys. 31 (1998) 1492.
[7] D. Zhang, T. Yoshida, H. Minoura, Chem. Lett. (2002) 874.
[8] T. Miyasaka, Y. Kijitori, T. N. Murakami, M. Kimura, S. Uegusa, Chem. Lett. (2002) 1250.
[9] H. Lindström, A. Holmberg, E. Magnusson, L. Malmqvist, A. Hagfeldt, J. Photochem. Photobiol. A 145 (2001) 107.
[10] K.P. Hanke, Zeitschrift fur Physikalische Chemie Bd. 212 (1999) 1.
[11] R. Kern, N. van der Burg, G. Chmiel, J. Ferber, G. Hasenhindl, A. Hinsch, R. Kinderman, J. Kroon, A. Mayer, T. Mayer, R. Niepmann, J. van Roosmalen, C. Schill, P. Sommering, M. Späth, I. Uhlendorf, Opto-Electron. Rev. 8 (4) (2000) 284.
[12] M. Späth, P.M. Sommeling, J.A.M. van Roosmalen, H.J.P. Smit, N.P.G. van der Burg, D.R. Mahieu, N.J. Bekker, M. Kroon, Prog. Photovolt. Res. Appl. 11 (2003) 207.
[13] G. Phani, M. P. J. Bertoz, J. Hopkins, I. L. Skryabin, G. E. Tulloch, Electric window modules based on nanocrystalline titania solar cells, Web document at http://www.sta.com.au/download/sol97ew.pdf.
[14] M. Grätzel, Prog. Photovolt. Res. Appl. 8 (2000) 171.
[15] M. Kurth, US Patent US6462266B1 (2002).
[16] T. Kawashima, H. Matsui, N. Tanabe, Thin Solid Films 445 (2003) 241.
[17] S. Ito, T. Kitamura, Y. Wada, S. Yanagida, Sol. Energy Mater. Sol. Cells 76 (1) (2003) 3.
[18] National Astronomical Observatory, Chronological Scientific Tables, Maruzen Co. Ltd., 1998, p. 527.